INVESTIGATIONS ON THE EFFECT OF HD PROCESSING IN LAND COVER CLASSIFICATION

I. Yalcin [1,2], G. Karakas [1,3], S. Kocaman [3, 4,*], S. Saunier [5], C. Albinet [6]

[1] Hacettepe University, Graduate School of Science and Engineering, Beytepe, Ankara, Turkey – <ilyas.yalcin><gizem.karakas>@hacettepe.edu.tr
[2] Hacettepe University, Baskent OSB Technical Sciences Vocational School, 06909 Sincan Ankara, Turkey
[3] Hacettepe University, Department of Geomatics Engineering, 06800 Beytepe Ankara, Turkey – sultankocaman@hacettepe.edu.tr
[4] ETH Zurich, Institute of Geodesy and Photogrammetry, 8093 Zurich, Switzerland
[5] Telespazio France, 26 Avenue Jean François Champollion, 31100 Toulouse - sebastien.saunier@telespazio.com
[6] European Space Agency, ESRIN, Via Galileo Galilei, 1, 00044 Frascati RM, Italy – clement.albinet@esa.int

Commission I, WG I/8

KEY WORDS: Image Classification, MAXAR HD, Land Use/Land Cover, Random Forest, Support Vector Machine

ABSTRACT:

The requirement of automated Land Use/Land Cover (LULC) classification has arisen in ecosystem related applications, such as natural hazard assessments, urban and rural area planning, natural resource management, etc. The data source and the classification method used in the production of LULC maps depend on the study area size and the location, and also determined by taking the time and cost into account. Recently, MAXAR Technologies announced a new product, High Definition (HD) with 15 cm resolution, which is obtained by post-processing of images with 30 cm Ground Sampling Distance (GSD). The post-processing employs machine learning methods. On the other side, the effect of HD processing on the image quality, and the usability of such products in various applications are still needed to be investigated. In this study, the influence of HD processing algorithm on LULC classification results was investigated by using 15 cm HD and 30 cm resolution images provided by MAXAR. By using the Random Forest (RF) and Support Vector Machine (SVM) methods in two different study areas, image classification was performed to detect water, vegetation, asphalt road, building, shadow, agriculture and barren land classes. The results show that in HD products, the edges of objects were sharper, whereas the classification noise was higher inside agricultural fields. Considering the overall results, it can be concluded that with the use of HD products in urban areas, improved LULC maps can be obtained.

1. INTRODUCTON

29% of the Earth's surface consists of lands, 71% of which are habitable areas. These areas can mainly be categorized as agriculture, forest, urban and roads (Our World in Data, 2021). The Land Use/Land Cover (LULC) maps have been frequently produced to aid the spatial planning of land as a non-renewable resource and to enable the sustainable development. The LULC maps have been employed in studies such as predicting biodiversity for the future (Niquisse et al., 2017), planning urban expansion areas (Rahman et al., 2012; Zhang et al., 2018), monitoring natural hazards (Karakas et al., 2021), etc.

With the help of developments in sensor and satellite technologies, the data needed for LULC studies can be obtained from Earth Observation (EO) data (Patra et al., 2018; Alqurashi and Kumar, 2019; Naikoo et al., 2020). Satellite optical images with high spatial resolution ensure regular data acquisition for LULC studies. The very high resolution (VHR) satellite images obtained by MAXAR Technologies are presented in High Definition (HD) quality with a Ground Sampling Distance (GSD) of 15 cm using a Machine Learning (ML) method (Blog MAXAR, 2021). The methodological details of this processing approach are yet unpublished. The MAXAR constellations cover more than 60% of the Earth's surface monthly, and have a 20-year data archive, which can be used for change detection studies (MAXAR, 2021).

The resolution improvement studies have recently gained a larger interest in the scientific community. With the approach, while the GSDs improve, several errors such as stair appearance on diagonal edges and blurring on the details and edges may occur (Van Ouwerkerk, 2006). Besides the conventional spatial and frequency domain methods, the deep learning techniques have a widespread use. A study by Zhu et al. (2021) has revealed that the use of satellite images obtained by a super resolution technique in LULC studies can increase the accuracy of classification. In a recent study by Yalcin et al. (2021) on the image quality evaluation of the HD products by using general image-quality equation (GIQE) metrics, sharper edges were observed. However, blurring, pattern noise, color deformations were also visible in high reflectance areas, such as desert.

The European Space Agency (ESA) aimed to cooperate between national space agencies as well as organizations engaged in commercial activities. For this purpose, the Earthnet Data Assessment Pilot (EDAP) project was developed by ESA (ESA, 2022). EDAP has established standards for performing early quality assessments on the data of national or commercial satellites. In this context, quality assessment procedures have been applied to several satellites such as Third Party Missions

* Corresponding author

(TPM), such as SkySat (Saunier et al., 2022). The MAXAR HD images were also evaluated within the EDAP context (e.g., see Yalcin et al., 2021). In order to gain further insights on the data and the potential applications, the data provided within the EDAP project was used here for carrying out further experiments on the HD data quality and usability.

In this study, the effect of MAXAR HD processing on LULC classification was investigated by comparing the results obtained from 15 cm HD and 30 cm pansharpened data in two different areas with urban and rural characters. The Random Forest (RF) and Support Vector Machine (SVM) algorithms, which are widely used in LULC studies (e.g., Pareeth et al., 2019; Balha et al., 2021; Karakas et al., 2021), were employed for this purpose. The datasets, the methodological details, results and discussions are presented in this paper.

2. MATERIALS AND METHODS

2.1 The Study Datasets

The satellite images used in the study were acquired from the WorldView-3 (WV3) satellite. The images are over the regions of Gibraltar and Novi Sad, Serbia. In both areas, multispectral (MS) images with both 15 cm and 30 cm resolutions were available as presented in Table 1. The images used in the study are pan-sharpened MS data. The products were delivered at Level 2 (LV2A), which indicates that the images are georeferenced to a projection system but not orthorectified (Digital Globe, 2014).

Study site	Date	Product Level	Bands	GSD
Gibraltar	24 Nov 2019, 11:33	LV2A	Pansharpened MS Bands	30 cm 15 cm
Novi Sad Serbia	28 Aug 2020, 09:48	LV2A	Pansharpened MS Bands	30 cm 15 cm

Table 1. MAXAR datasets used in LULC map production.

The Novi Sad region is in the Balkan lands of Serbia. The Gibraltar test site is located on the Mediterranean coast (Figure 1). In the study, the Gibraltar region was mainly used for the classification of urban areas and water bodies, while the Novi Sad Serbia region was preferred for its agricultural land cover.

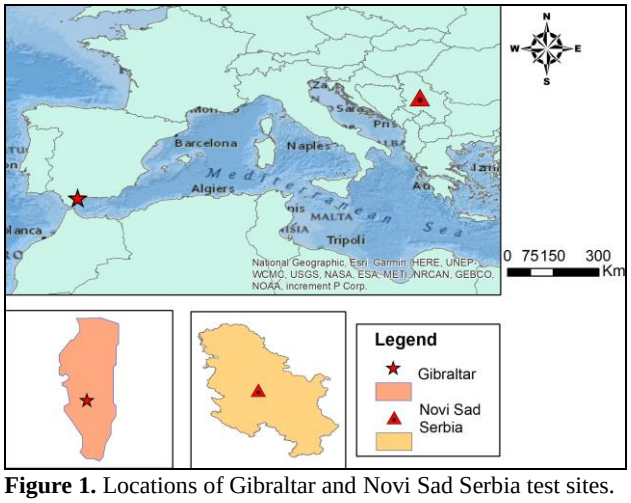

Figure 1. Locations of Gibraltar and Novi Sad Serbia test sites.

2.2 Methodology

2.2.1 The Overall Workflow: In this study, the image classification was performed using two different ML techniques, i.e., the SVM and the RF. The overall workflow of the study is illustrated in Figure 2. The original pansharpened MS and HD images of both sites were classified by using both methods and after a tiling process. The validation of the results was performed by using statistical parameters and visual inspection of the final LULC maps.

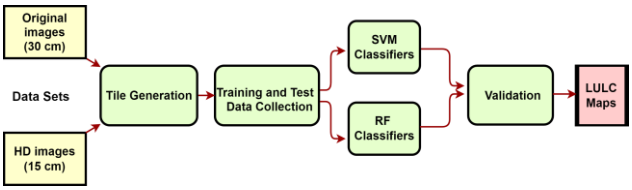

Figure 2. The overall workflow of the study.

2.2.2 Training Data Selection: In the study, the satellite images were first divided into tiles in order to optimize the computations. At this stage, the pansharpened and the HD images of Gibraltar were divided into 4 equal tiles (Figure 3). Examples to training polygons selected in this region (marked with a-d in Figure 3) are presented in Figure 4. The Novi Sad images were divided into 2 equal areas (Figure 5) and examples views are presented in Figure 6. The LULC classes defined in Gibraltar images include water, vegetation, asphalt, shadow, buildings with roof tiles (building-1/ with tile colour), buildings without roof tiles (building-2/light colour), and barren land. In the Novi Sad site, the defined classes are three types of vegetated land (i.e., vegetation-1, vegetation-2, vegetation-3), wooded area and roads. The classes in both sites were identified based on the dominant land cover types; and the object types with a small number of pixels or rare appearances in the images (e.g., ships) were not considered.

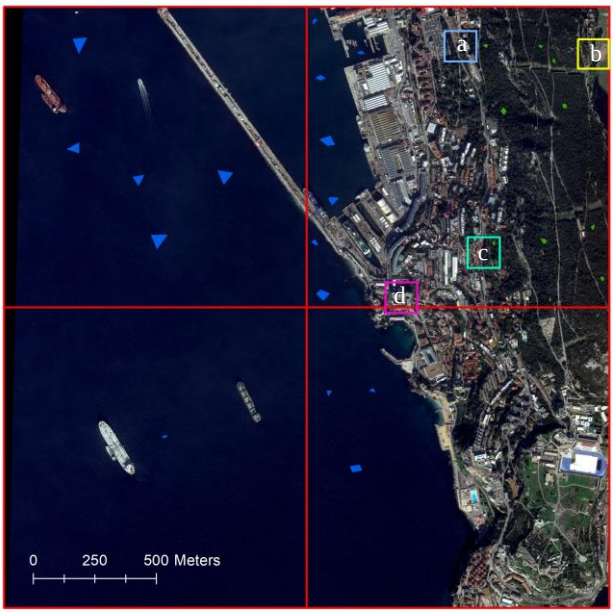

Figure 3. MAXAR image of Gibraltar test site, the tiles used for classification, test data polygons and location. The tile numbers are: tile-0 (top left), tile-1 (top right), tile-2 (bottom left), tile-3 (bottom right).

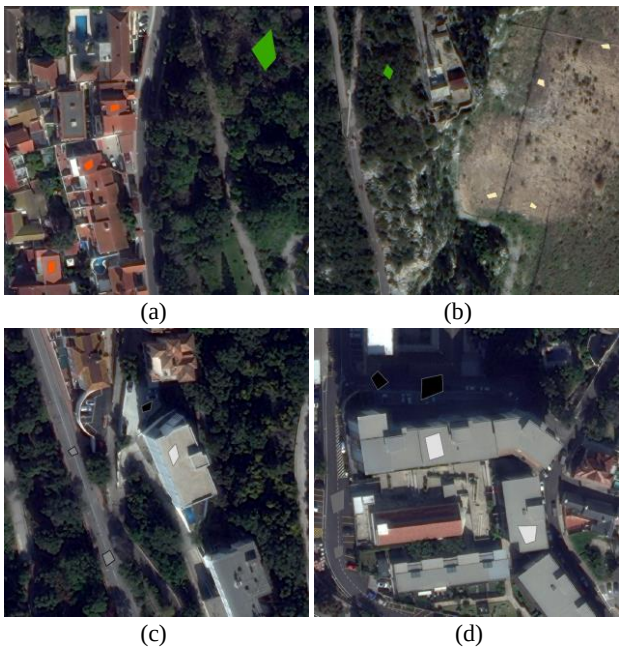

Figure 4. Sample training polygons defined on MAXAR image of Gibraltar test site. (a) Building_1 and vegetation, (b) vegetation and barren, (c) building_2 and (d) building_2 and shadow.

Figure 5. MAXAR image of Novi Sad test site and the tiles used for classification, training polygons and location. The tile numbers are: tile_0 (left) and tile_1 (right).

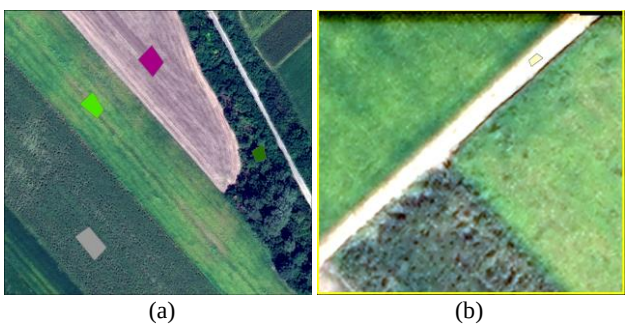

Figure 6. Sample training polygons defined on MAXAR image of Novi Sad test site with locations shown on Figure 5. (a) vegetation-1, vegetation-2, vegetation-3, wooded area, (b) road.

In the training and test data collection stage, tile-1 (top right tile in Figure 3) was used in Gibraltar test site as it included samples for all classes. The test data was collected from all tiles in Gibraltar. In total of 470,328 training data samples (pixels) and 759,391 test samples were selected for the model training and quality assessment from the 30 cm images. In Novi Sad, the number of training and test samples collected in the 30 cm image were 149,523 and 75,618, respectively. The training samples were collected in tile-0 (left tile in Figure 5) in Novi Sad and the test samples were collected in both tiles. The same training and test polygons were applied to the HD images, which resulted in higher numbers of samples for both sites. The training and test samples were selected carefully by comparing the 30 cm data by overlapping in the 15 cm data to obtain the most representative samples in both.

The RF and SVM models were trained using the training samples in tile-1 in Gibraltar as it included all classes. The trained RF model was applied to all tiles to produce the final LULC map. However, the SVM model was applied only to the trained tile (tile-1) to provide a comparison with the RF results.

2.2.3 The ML Classifiers: After the data preparation, the image classification stage was carried out. The RF and the SVM algorithms were found to be successful in the production of LULC maps in image classification studies (Zhang et al., 2018). In addition, among the image classification methods used in 349 peer-reviewed journals analysed by Tamiminia et al. (2020) based on the Google Earth Engine (GEE) platform, the RF was preferred with a high rate of 49% and the SVM with 11%. In addition, although novel deep learning methods including convolutional neural networks could be employed for the LULC classification, they require a greater amount of training data depending on the number of bands, the number of classes, spatial resolution and platform of the data (Shendryk et. al. 2019; Debella-Gilo et. al. 2021). Therefore, the RF and the SVM techniques were preferred in the production of LULC maps in this study.

The RF is a non-parametric ML algorithm. Its working principle is based on the decision tree (DT) (Breiman, 2001). The main purpose of the DT method is to reduce high variance values. For this purpose, the training data is analysed based on bootstrapped samples and the average of estimate is considered as final output data. The RF is more powerful than the other DT methods such as bagging and boosting since the subsets for each tree independently generate the prediction result. The determination of the hyperparameters while creating the RF model is of high significance for obtaining high accuracy in the classification. In this study, the scikit-learn library was used for applying the RF model (Scikit-learn, 2021). The RandomizedSearchCV function was used to determine the hyperparameters of the RF model (RandomizedSearchCV, 2021). The difference of this cross validation method from the GridSearchCV method is that it searches for hyperparameters among the parameters with specified boundaries rather than all parameters. Therefore, the computational cost is also reduced. The hyperparameter values obtained during the optimization process of the 15 cm HD and 30 cm pansharpened data in the RF model are shown in Table 2. The validation of the RF results was provided with the test data collected from all tiles. Furthermore, for the validation of the RF, the out-of-bag (OOB) method, which allows estimating these data for each tree by separating 1/3 of the training data (James et al., 2013), was used.

The SVM is also a ML algorithm that can perform a non-parametric supervisor classification proposed by Cortes and Vapnik (1995). The classification studies can also be performed with linear estimation methods. However, the linear methods

may be less successful in some data sets. Therefore, linear methods involve expanding the feature space. In this way, the classification studies can be carried out as in the non-linear methods. The SVM, on the one hand, becomes a non-linear method by expanding feature space with a kernel-based approach. In the SVM method, the most appropriate hyper plane can separate the two classes. The hyper plane, which is determined as the highest distance between the two classes of hyper plane, is the ideal plane that can be used to separate these classes. This maximum space is called the margin and the data limiting these spaces is called the support vector (Oommen et al., 2008; Dtreg, 2021). In this study, the SVM classifier was implemented using ENVI 5.0 software (ENVI, 2021). The kernel type for the 15 cm HD and 30 cm pansharpened data is given in the SVM model in Table 2. The train and test data implemented for the RF classifier were also used in the SVM method.

Model	Hyperparameter	Gibraltar		Novi Sad	
		15 cm HD	30 cm	15 cm HD	30 cm
RF	n_estimators	263	312	312	385
	criterion	entropy	gini	entropy	entropy
	max_depth	50	50	16	27
	min_samples_split	10	10	8	2
	min_samples_leaf	2	2	1	1
	max_feature	sqrt	auto	sqrt	auto
SVM	Kernel type	Radial Basis (Gaussian) Function			

Table 2. Model parameters employed in the study.

3. RESULTS AND DISCUSSIONS

Here, the MAXAR WV3 satellite images with 30 cm and 15 cm resolutions were classified by using the RF and the SVM methods. The RF model was trained in one tile and applied to the other tiles. The same training and validation data samples were used for both methods. The results are presented under the following subheadings.

3.1 The Random Forest Results

The RF classification results (i.e., LULC maps) of 15 cm HD images of Gibraltar and Novi Sad Serbia regions are presented in Figures 7 and 8. The RF model results applied to all tiles belonging to Gibraltar and Novi Sad test sites are given in Table 3. Since the Novi Sad site consists of 2 tiles, the other tiles are shown as No Data in the table.

The overall accuracy (OA) of the RF model was found to be high in both study regions. For Gibraltar, tile-0 and tile-2 are predominantly water bodies while tile-1 and tile-3 include the city areas, artificial facilities and green spaces. The lower OA values in HD products in tile-2 (mainly water and shadow areas) can be associated with the higher noise level in these images. In the Gibraltar region, the water class and the coastlines are detected better with 15 cm HD images (see Figure 9). In the image with 30 cm GSD, there are interferences between shadow and water, barren and building-1 classes. Moreover, mis-classifications and lower accuracy were observed in asphalt and building-2 fields in both 15 cm HD and 30 cm images. However, in the HD images, the water class was distinctively separated from the other classes. Considering the fact that tile-3 is the best test area for the Gibraltar site, it can be observed in Table 3 that the HD data provided better prediction performance. The 30 cm yielded higher accuracy with the test tile (tile_0) in Novi Sad, although the difference is relatively small (0.9%).

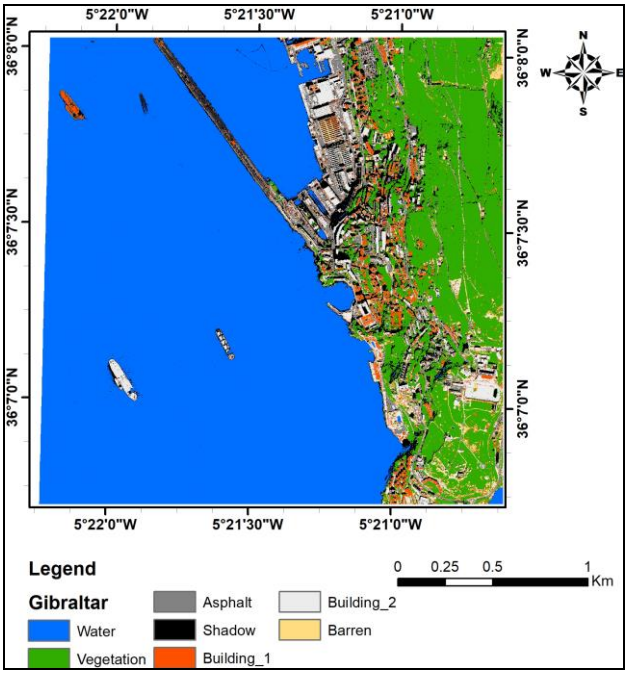

Figure 7. The RF classification result of Gibraltar MAXAR HD image.

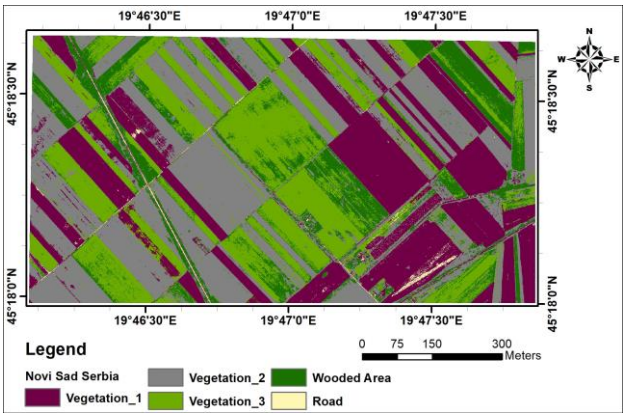

Figure 8. The RF classification result of Novi Sad Serbia MAXAR HD image.

Random Forest	Overall Accuracy			
Image Name	Tile-0	Tile-1	Tile-2	Tile-3
Gibraltar 15 cm HD	99.0%	98.7%	92.5%	97.0%
Gibraltar 30 cm	98.8%	98.0%	99.0%	93.4%
Novi Sad 15 cm HD	97.3%	99.3%	No Data	No Data
Novi Sad 30 cm	98.2%	98.0%	No Data	No Data

Table 3. The overall accuracy values obtained from the RF model results for all tiles in both sites.

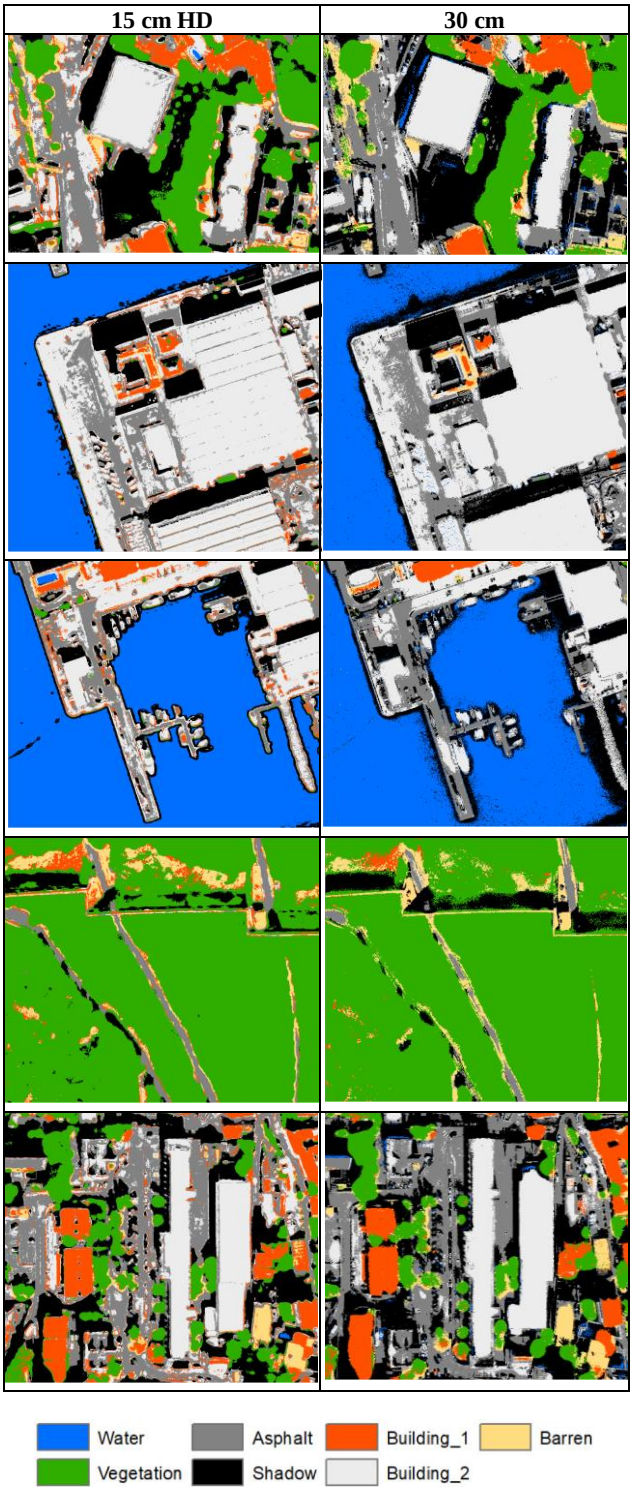

Figure 9. Image parts containing 15 cm HD and 30 cm RF model results in the Gibraltar region

A number of classification examples from the RF model trained in Novi Sad site are presented in Figure 10. In the classification study carried out in the agricultural region, the borders of the crop fields were obtained sharply in the 15 cm HD image. However, the HD image shows a noisy structure within the agricultural areas. Images with 30 cm GSD produced a smoother class output. On the other hand, the field boundaries in these images appear to be less straight when compared with the 15 cm HD output.

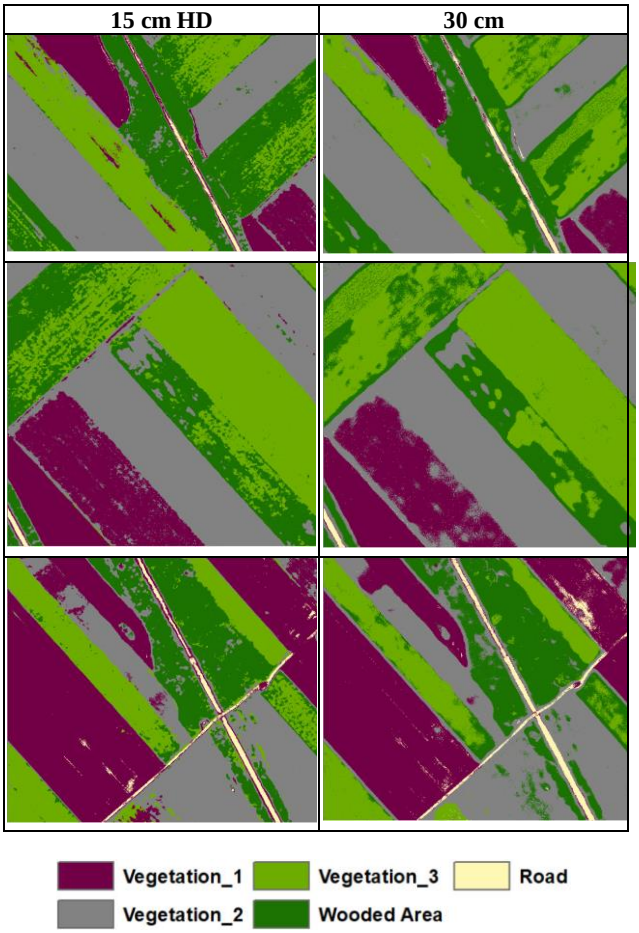

Figure 10. Image parts containing 15 cm HD and 30 cm RF model results in the Novi Sad site.

3.2 The SVM Results

The SVM model used in the study was trained with the tile-1 of Gibraltar images and the tile-0 of Novi Sad images. Table 4 illustrates SVM results from the training tiles based on the OOB method. Similar to the RF results, the HD images provided higher accuracy for Gibraltar. In Novi Sad, the overall accuracy values obtained from both images are similar.

Support Vector Machine	Overall Accuracy	
Image Name	**Tile-0**	**Tile-1**
Gibraltar 15 cm HD	No Data	95.0%
Gibraltar 30 cm	No Data	92.6%
Novi Sad 15 cm HD	98.0%	No Data
Novi Sad 30 cm	97.4%	No Data

Table 4. The overall accuracy values obtained from the SVM model results for all tiles in both sites.

A number of examples from the SVM classification results in the Gibraltar region are presented in Figure 11. The same regions as in Figure 9 were selected and presented for visual comparison.

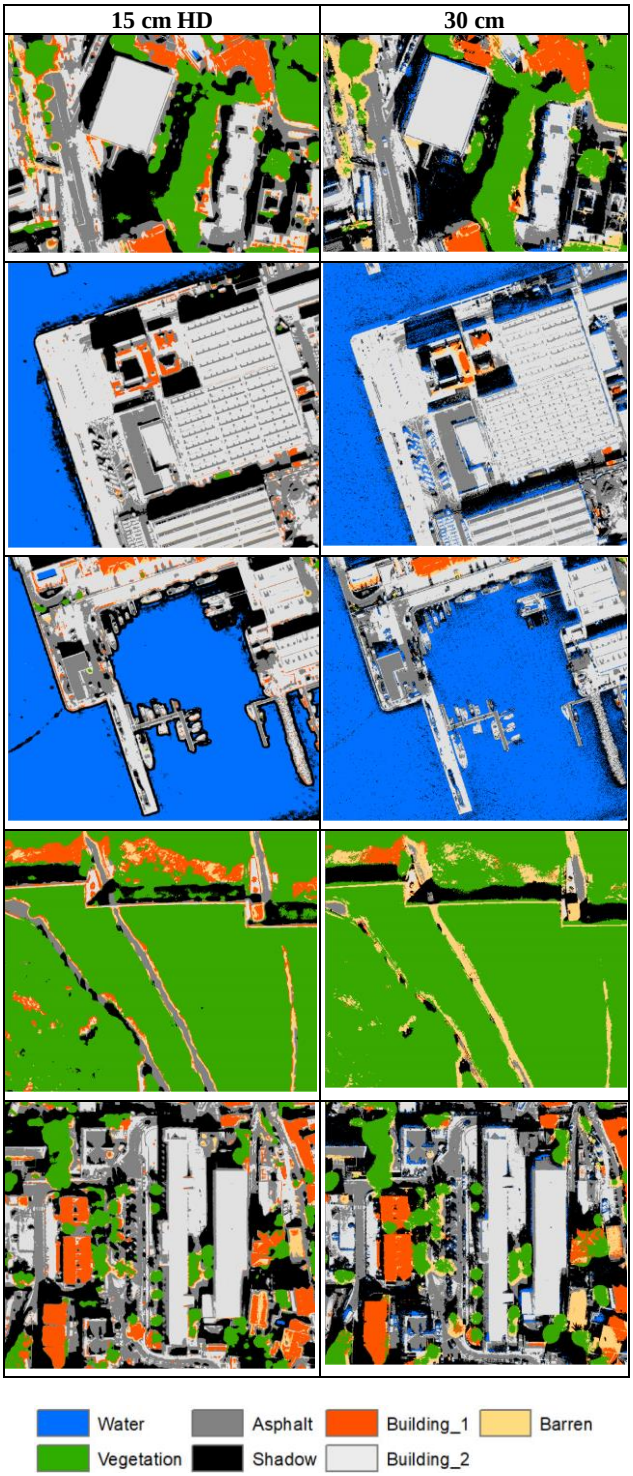

Figure 11. Image parts containing 15 cm HD and 30 cm SVM model results in the Gibraltar region

The SVM has achieved high-accuracy classification results similar to the RF model. In addition, the SVM also produced some classification errors. In some areas in the 15 cm HD image, the SVM provided higher sharpness on the edges than the RF model. However, as in the RF model, the spectral overlap between water fields and shadow classes was detected in SVM. Furthermore, building-2 and asphalt classes have more spectral interference compared to the RF model. However, the sharpness of the edges is higher than the RF model.

Sample image parts similar to the areas in the RF model results (see Figure 10) in Novi Sad Serbia are presented in Figure 12. Similar to the RF model, the sharpness of the edges of agriculture regions in 15 cm HD images is better than the images with the 30 cm GSD. The formation of spectral blending in the classification results within the agricultural fields is also seen in the SVM model results. The edge improvement was evaluated quantitatively using a Modulation Transfer Function (MTF) target by Yalcin et al. (2021).

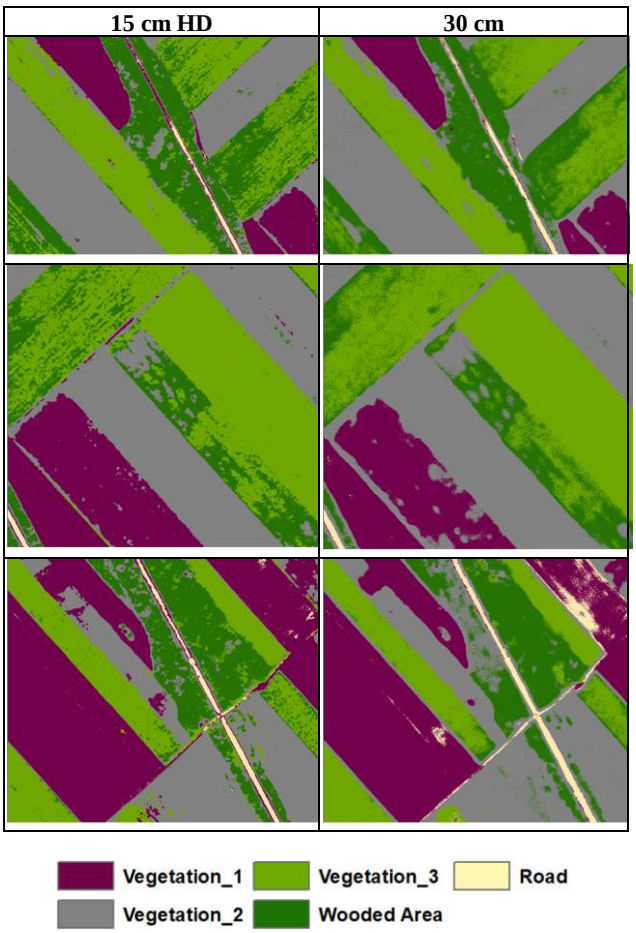

Figure 12. Image parts obtained from 15 cm HD and 30 cm SVM model results in Novi Sad site.

According to all classification results obtained in the study, interferences were detected between classes in areas with the same pattern in the HD images. At the same time, the HD images provided very accurate results in the detection of coastlines. In agricultural areas, classification results exhibited problems in HD images due to the blending of fields. However, the HD image allows the agriculture borders to be produced more clearly than the image with 30 cm GSD.

Yalcin et al. (2021) evaluated the radiometric quality of MAXAR HD products using the GIQE criteria, visual evaluation and orthophotos produced from Unmanned Aerial Vehicle (UAV) data. It was emphasized in their study that MAXAR HD products produced Gaussian noise and blurring during the super resolution process while improving their GSDs. In the light of this information, it can be concluded that the errors observed in the classification study, especially inside the crop fields, are caused by Gaussian noise in the image. It

can also be said that moderation at the diagonal edges in urban areas positively affects the production of the coastlines in the classification on 15 cm HD images. The edge improvement can be quantitatively evaluated by using natural targets as future work.

4. CONCLUSIONS

In this study, the quality comparison between the LULC maps produced from the images of MAXAR satellites through image classification was performed by analysing the influence of the HD products on the results. For this purpose, pansharpened MS WV-3 images provided by MAXAR Technologies and the HD images produced from these images by applying ML techniques were used. The original and the HD images were classified using the RF and SVM models and the results were compared. The overall accuracy values obtained from both methods in two different sites, one with urban and the other one with agricultural characteristics, range between 92.6% - 99.0%. Although both methods provided comparable prediction performances with the test data, the RF provided smoother class structures. The SVM was however better to detect small details, such as on the roofs.

The image quality improvement of the HD products were mainly observable in urban areas with strong edges, which demonstrates a clear advantage for LULC classification in urban areas. In the agricultural areas, although the field boundaries were mapped better with the HD images, a smoother classification was made inside the fields by using the original images. Image filters can be used to smoothen the noisy classification encountered with the HD products in agricultural areas.

Thanks to the developments in hardware technology and the deep learning techniques, it can be expected that the number of image quality and resolution improvement studies will increase. Thus access to high-resolution images will become easier that are beneficial for various applications.

ACKNOWLEDGEMENTS

This contribution was funded by the ESA Earthnet Data Assessment Pilot (EDAP) project (Optical Cluster) (https://earth.esa.int/eogateway/activities/edap). The authors are grateful to MAXAR Technologies for the provision of satellite imagery. İlyas Yalçın and Gizem Karakaş acknowledge the support of the Scientific and Technological Research Council of Turkey (TUBITAK) 2224-A Grant Program for Participation in Scientific Meetings Abroad.

REFERENCES

Alqurashi, A.F., Kumar, L., 2019. An assessment of the impact of urbanization and land use changes in the fast-growing cities of Saudi Arabia. *Geocarto International*, 34(1), 78-97, DOI: 10.1080/10106049.2017.1367423.

Balha, A., Mallick, J., Pandey, S. et al. 2021. A comparative analysis of different pixel and object-based classification algorithms using multi-source high spatial resolution satellite data for LULC mapping. *Earth Sci Inform*, 14, 2231–2247. DOI: 10.1007/s12145-021-00685-4.

Blog MAXAR, 2021. https://blog.maxar.com/earth-intelligence/2020/hd-satellite-imagery-and-machine-learning-more-accurately-detect-and-locate-features-of-interest-with-greater-consistency. (last accessed on 28 Dec 2021).

Breiman, L., 2001. Random Forests. *Machine Learning*, 45, 5–32.

Cortes, C., Vapnik, V., 1995. Support Vector Networks. *Machine Learning*, 20, 273-297. DOI:10.1007/BF00994018.

Debella-Gilo, M., Gjertsen, A.K., 2021. Mapping Seasonal Agricultural Land Use Types Using Deep Learning on Sentinel-2 Image Time Series. *Remote Sensing*, 13 (2), 289. DOI:10.3390/rs13020289.

Digital Globe, 2014. Imagery Support Data (ISD) Documentation v.1.1.2. October. 73p.

Dtreg, https://www.dtreg.com/solution/support-vector-machines. (last accessed on 28 Dec 2021).

European Space Agency (ESA), 2022. https://earth.esa.int/eogateway/activities/edap (last accessed on 17 January 2022)

ENVI 5.0 L3HARRIS GEOSPATIAL, 2021. https://www.l3harrisgeospatial.com/Support/Self-Help Tools/Help-Articles/Help-Articles Detail/ArtMID/10220/ArticleID/18216/5234 (last accessed on 29 December 2021).

James, G., Witten, D., Hastie, T., Tibshirani, R., 2013. *An Introduction to Statistical Learning*. Springer.

Karakas, G., Nefeslioglu, H.A., Kocaman, S., Buyukdemircioglu, M., Yurur, M.T., Gokceoglu, C., 2021. Derivation of earthquake-induced landslide distribution using aerial photogrammetry: the 24 January 2020 Elazig (Turkey) Earthquake. *Landslides*, 18, 2193-2209. DOI:10.1007/s10346-021-01660-2.

MAXAR, 2021. https://www.maxar.com/constellation (last accessed on 29 Dec 2021)

Naikoo, M.W., Rihan, M., Ishtiaque, M., Shahfahad, 2020. Analyses of land use land cover (LULC) change and built-up expansion in the suburb of a metropolitan city: Spatio-temporal analysis of Delhi NCR using landsat datasets. *Journal of Urban Management*, 9(3), 347-359. DOI:10.1016/j.jum.2020.05.004.

Niquisse, S., Cabral, P., Rodrigues, Â., Augusto, G., 2017. Ecosystem services and biodiversity trends in Mozambique as a consequence of land cover change. *International Journal of Biodiversity Science, Ecosystem Services & Management*, 13(1), 297-311. DOI:10.1080/21513732.2017.1349836.

Oommen, T., Misra, D., Twarakavi, N.K.C. et al., 2008.An Objective Analysis of Support Vector Machine Based Classification for Remote Sensing. *Math Geosci*, 40, 409–424. DOI:10.1007/s11004-008-9156-6.

Our world in data, 2021. https://ourworldindata.org/land-use (last accessed on 29 Dec 2021).

Pareeth, S., Karimi, P., Shafiei, M., De Fraiture, C., 2019. Mapping Agricultural Landuse Patterns from Time Series of

Landsat 8 Using Random Forest Based Hierarchial Approach. *Remote Sens.*, *11*, 601. DOI:10.3390/rs11050601.

Patra, S., Sahoo, S., Mishra, P., Mahapatra, S.C., 2018. Impacts of urbanization on land use /cover changes and its probable implications on local climate and groundwater level. *Journal of Urban Management*, 7(2), 70-84. DOI:10.1016/j.jum.2018.04.006.

Rahman, A., Kumar, S., Fazal, S., Siddiqui, A.A., 2012. Assessment of Land use/Land cover Change in the North-West District of Delhi Using Remote Sensing and GIS Techniques. *Journal of Indian Society of Remote Sensing*, 40(4), 689-697. DOI:10.1007/s12524-011-0165-4.

RandomizedSearchCV, 2021. https://scikit-learn.org/stable/modules/generated/sklearn.model_selection.RandomizedSearchCV.html (last accessed on 29 Dec 2021).

Saunier, S., Karakas, G., Yalcin, I., Done, F., Mannan, R., Albinet, C., Goryl, P. and Kocaman, S., 2022. SkySat Data Quality Assessment within the EDAP Framework. *Remote Sensing*, 14(7):1646. DOI:10.3390/rs14071646.

Scikit-learn, 2021. Python Library. https://scikit-learn.org/stable/modules/generated/sklearn.ensemble.RandomForestClassifier.html (last accessed on 29 Dec 2021).

Shendryk, Y., Rist, Y., Ticehurst, C., Thorburn, P., 2019. Deep learning for multi-modal classification of cloud, shadow and land cover scenes in PlanetScope and Sentinel-2 imagery. *ISPRS Journal of Photogrammetry and Remote Sensing*, 157, 124-136. DOI: 10.1016/j.isprsjprs.2019.08.018.

Tamiminia, H., Salehi, B., Mahdianpari, M., Quackenbush, L., Adeli, S., Brisco, B., 2020. Google Earth Engine for geo-big data applications: A meta-analysis and systematic review. *ISPRS Journal of Photogrammetry and Remote Sensing*, 164, 152-170. DOI:10.1016/j.isprsjprs.2020.04.001.

Van Ouwerkerk, J.D., 2006. Image super-resolution survey. *Image and Vision Computing*, 24(10), 1039-1052. DOI:10.1016/j.imavis.2006.02.026.

Yalcin, I., Kocaman, S., Saunier, S., Albinet, C., 2021, Radiometric Quality Assessment for Maxar HD Imagery. *The International Archives of Photogrammetry, Remote Sensing and Spatial Information Sciences*, XLIII-B3, 797-804. DOI:10.5194/isprs-archives-XLIII-B3-2021-797-2021

Zhang, P., Ke, Y., Zhang, Z., Wang, M., Li, P., Zhang, S. 2018. Urban Land Use and Land Cover Classification Using Novel Deep Learning Models Based on High Spatial Resolution Satellite Imagery. *Sensors*, 18, 3717. DOI:10.3390/s18113717.

Zhu, Y., Geiß, C., So, E., 2021. Image super-resolution with dense-sampling residual channel-spatial attention networks for multi-temporal remote sensing image classification. *International Journal of Applied Earth Observation and Geoinformation*, 104, 102543. DOI:10.1016/j.jag.2021.102543.